Research Article

Mapping Geotechnical Soil Properties of Ranya City in Kurdistan Region of Iraq Using GIS

Bashdar Omer [a,*], Shwana Manguri [b], Araz Hamza [c]

Department of Civil Engineering, University of Raparin, Ranya, Sulaymaniyah, Kurdistan Region, Iraq

[a] bashdar.omer@uor.edu.krd, [b] shwana.manguri@uor.edu.krd, [c] araz.hamza@uor.edu.krd

Access this article online		
Received on: 31 March 2022	**Accepted on:** 15 May 2022	**Published on:** 30 June 2022
DOI: 10.25079/ukhjse.v6n1y2022.pp69-83	**E-ISSN:** 2520-7792	

Abstract

Geotechnical map is a vital guidance to visualize the behavior of soils. The objective of this paper is to present the geotechnical maps that can be used for preliminary investigation in Ranya city of northern Iraq. The study area is 13.02 km² with latitude and longitude of 36°15'14" N 44°52'59" E, respectively. A total number of 116 boreholes with the depth up to 5.0 m were utilized to create allowable bearing capacity, particle size, and Atterberg limit maps. Kriging interpolation tool in the ArcGIS software was used to analyze the soil properties data and to achieve the maps. The appraisal study area was divided into three layers 0.5-1.5, 1.5-3.0, and 3.0-5.0 m and the results show the average bearing capacity of 112.2, 168.5, and 244.2 kN/m² sequentially. Moreover, Particle size distribution's results illustrate that gravel percentage increases in the deeper layers, while fines content decreases with no significant change of sand content. In addition, very high bearing capacity areas were mostly found in the southern and northern parts of the studied area. However, the eastern area represents the area with the minimum bearing capacity where it gradually increases toward the west. Furthermore, the liquid limit and plasticity index reduce from the north to south with an increase in depth of the layers from 3.0-5.0 m. The highest liquid limit value is observed in the depth of 1.5-3.0 m.

Keywords: Atterberg Limit Map, Bearing Capacity Map, Geotechnical Map, GIS, Particle Size Map.

1. Introduction

Rapid population growth demands more residential areas for settlement. In the past 15 years, the population of Ranya district has increased rapidly by 60 % (Annual population statistical report, 2021). This population rise increases the need for building more residential areas and engineering projects, for which site investigation of the soil is essential which is a difficult task that requires substantial effort, time and cost.

Using technology can save time and cost of the investigations if used correctly. With the developments in computation in the last two decades, GIS is often used to capture, store, manage, query, analyze, display and retrieve huge volumes of referenced geospatial data and associated attribute data collected from variety of sources (Manguri and Hamza, 2021; Mirzahossein et al., 2020; Tripathi et al., 2021). GIS provides data with actual geographical location. It has a significant role in geotechnical engineering, for instance; generating and visualizing data of inaccessible locations with the aid of interpolation techniques and representing the analyzed data by means of digital maps, graphs, and charts (Singh et al., 2015). In addition, GIS multifunctional features especially spatial and statistical operations can be used to perform analysis

and visualize types of composites in hard and soft copy formats such as images, notices, borings, geotechnical properties of soils, and other site-specific data.

Many researchers tried to create GIS maps for a local area such as; (Jimenez et al., 2000) investigated hazards map prediction of Barcelona in Spain that revealed predominant period, amplification ratio and geology maps. In addition, (Valverde-Palacios et al., 2014) demonstrated a geotechnical map of foundation conditions for Granada in Spain based on properties of soils such as standard penetration value, bearing capacity, cohesion, internal friction angle, bulk density, particle size, groundwater table condition and minimum foundation depth. The problematic and expansive soil layer maps of the Toshka region in Egypt and Surfers Paradise in Australia were determined by (Labib and Nashed, 2013) and (Al-Ani et al., 2013) respectively. Other researchers investigated some physical and mechanical properties. For example, some of municipal districts of Tehran in Iran are presented by digital maps (Razmyar and Eslami, 2016, 2018). (El-Kady and ElMesmary, 2018) explored and formed a database for soil and rock types of 12 m below ground surface and interpolated the data using GIS to create a bearing capacity map of the Sakaka area in Saudi Arabia. (Kaur et al., 2019) calculated bearing capacity mapping of Srinagar, Jammu and Kashmir utilizing 39 boreholes.

(Kamal et al., 2016) and (Khalid et al., 2021) developed geotechnical map zones of Pakistan based on standard penetration values for Faisalabad and Islamabad. Also, (Arshid and Kamal, 2020) exposed soil classification, bearing capacity and AASHTO subgrade rating at different depths for Potohar plateau in Pakistan. (Celik et al., 2021) presented and investigated geological and geotechnical data for Nigde city in Turkey dividing the area to five regions. They plotted standard penetration values, bearing capacity, liquefaction zone, soil classification and plasticity index maps. (Cabalar et al., 2021) investigated Erzincan city near north Anatolian fault zone in the eastern Turkey, a series of geotechnical maps based on data from 92 boreholes were produced. The maps included water content, Atterberg limits, soil classification, standard penetration test, shear wave velocity, and primary wave velocity. Also, a relationship between the unconfined compression testing results and dynamic elastic modulus was achieved by neural network.

Some other researchers demonstrated the physical and mechanical properties of soil by producing digital maps in the middle and south of Iraq, for instance; (Kadhim et al., 2013) focused on distributed geotechnical properties of Basrah City through presenting bearing capacity, undrained shear strength, liquidity index and compression index maps at different depths. (Kadhim and Al-Abody, 2015) created bearing capacity maps to residential areas for every 1.5 m of depth up to the depth of 10 m of Al-Imam district in Babil, Iraq. Similarly, (Al-Maliki et al., 2018) showed the bearing capacity map of An-Najaf and Kufa cities at depths of 0-2 m with ranges of 5-20 Ton/m^2. Also, (Aldefae et al., 2020) created digital geotechnical parameters including bearing capacity, coefficient of consolidation, compression index, swell index, cohesion, angle of friction and groundwater level for Wasit province, Iraq, using 164 borehole logs distributed over 17000 km^2 studied area with the range of the depth is 0-10 m. (Ali and Shakir, 2021) studied soil characteristics in ThiQar Governorate, Iraq, based on 423 boreholes distributed over an area of 12900 km^2. They drew geotechnical maps comprised of water content, dry density, liquid limit, specific gravity, standard penetration test, groundwater and ultimate bearing capacity maps. In Salah Al-Deen, digital maps were produced by (Mohammed et al., 2020) representing the distribution of soil classification, bearing capacity, standard penetration test and chemical properties of the soil. Meanwhile, (Al-Mamoori et al., 2020) created unified soil classification system, and coarse and fine grained maps using 464 boreholes for An-Najaf city at depths of 0-26 m covering an area of approximately 105.1 km^2. Additionally, researchers have studied characteristics of soil properties in Sulaimani governorate in the north of Iraq, (Najmaddin et al., 2020; Rashed and Hussein, 2020). Physical and mechanical soil characteristics of Sulaimani city have been studied by using ArcGIS for characterization and modeling purpose based on the experimental and literature data (Ahmed et al., 2020).

In accordance with the literature data, geotechnical maps were created for different places in Iraq, which are vital for construction process. However, there is no such a geotechnical map which was studied for Ranya district, and it is considered as a research gap. Since soil investigation is costly and cannot be done for every small project, the engineers and designers need to assume some geotechnical parameters of the soil especially bearing capacity value. As a reasonable solution for the issue of lack of similar research in the study area, the authors of this study collected and used the available data from technical reports to create geotechnical maps for different soil properties of Ranya city. Similar to other studies found in the literature, this study has used GIS as a tool for producing the maps. However, the study tries to cover most of soil properties including the bearing capacity. Also, it tries to utilize more borehole data to represent the maps accurately.

2. Study Area

Ranya district is located in Sulaymaniyah governorate, Kurdistan Region, Iraq, with latitude and longitude of 36°15'14"N 44°52'59"E respectively. It is located in the north west of Sulaymaniyah city as shown in Figure 1. Its elevation is about 615 m with respect to the MSL. Ranya is approximately 104 km away from Sulaymaniyah city center (Bapeer et al., 2020).

The area of Ranya municipality is about 27.15 km² while the study area is only 13.02 km² which is part of most populated area of the city. Structurally, Ranya is located in the boundary between highly folded zone and imbricated zone (Jassim and Goff, 2006). Geologically, the district area is covered by alluvial sediments, which consist of gravel, sand, silt, and clay (Bapeer et al., 2020; Sissakian, 2000). The groundwater table ranges between (20-40) m below the ground surface (Al-Jiburi and Al-Basrawi, 2015; Al-Manmi, 2008). The city is surrounded by two mountains namely; Kewerash from the north, Hajila from the west, and Dokan lake from the south. Ranya climate belongs to Mediterranean system climate so, its winter is cold and wet while its summer is hot and dry (Khdir and Saeed, 2021).

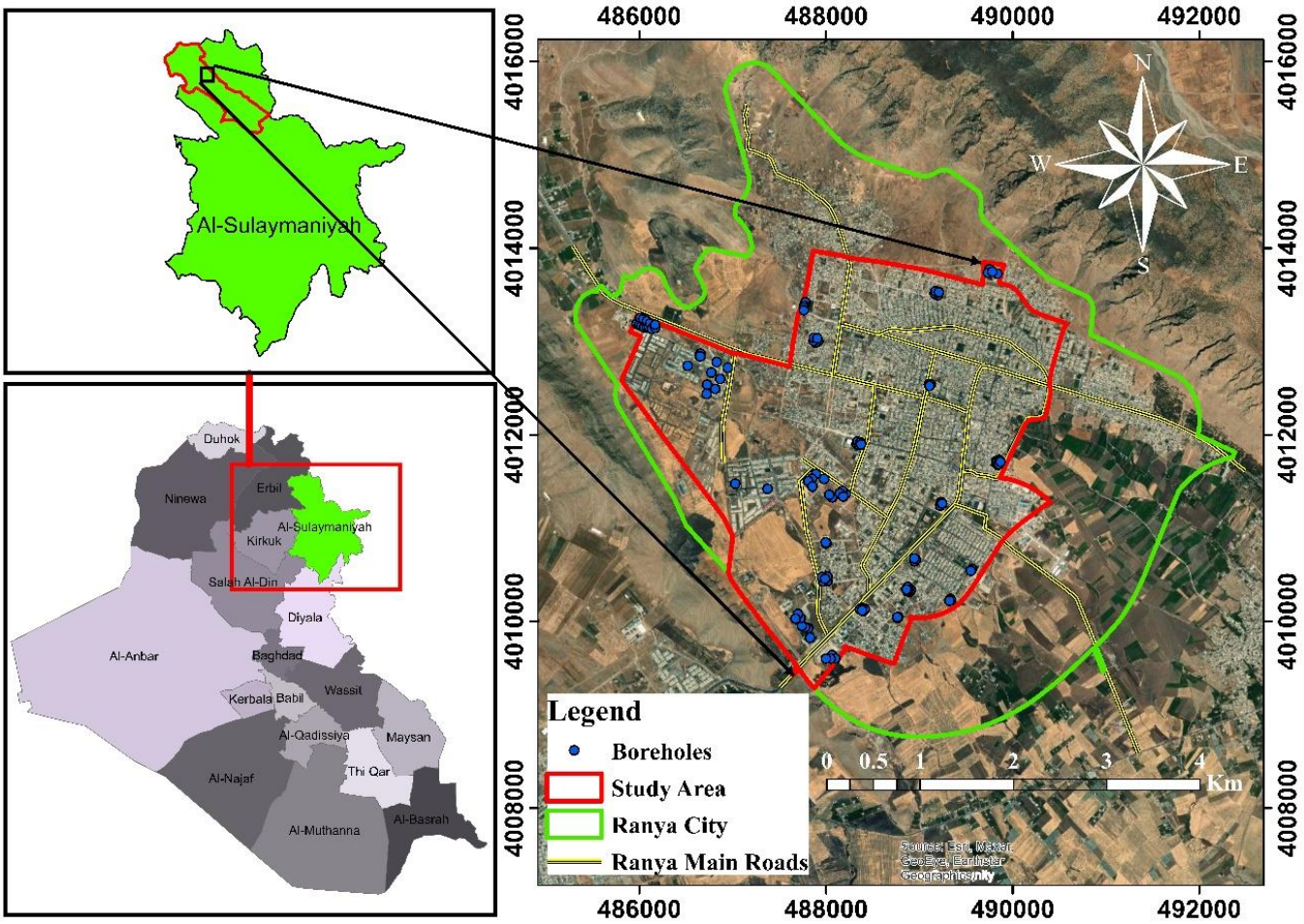

Figure 2. Ranya City in The Iraqi Map (Study Area).

3. Methodology

3.1. Data Collection

Geotechnical investigation reports were collected from 26 sites providing data of 116 boreholes distributed over the study area. The tests were carried out by consultant engineering bureaus (Consultant Engineering Bureau of Sulaimani University; Seko Private Construction Lab; Sulaymaniyah General Construction Lab). The data were implemented for infrastructure projects of Ranya municipality boundary. The boreholes range up to 5 m. From each of the boreholes, disturbed and undisturbed samples were collected for performing tests to determine mechanical properties of soil according to the ASTM standards. The extracted data from the reports were Atterberg limits ASTM D4318 (ASTM, 2010), particle size analysis ASTM D422-63 (ASTM, 2007), unit weight ASTM D7263 (ASTM D7263, 2018), standard penetration test ASTM D1586 (ASTM D1586-11, 2011) and dynamic cone penetrometer ASTM D6951 (ASTM D

D6951, 2003). The study area was divided into three layers with depths ranging between 0.5-1.5, 1.5-3.0, and 3.0-5.0 m. For each layer, liquid limit (LL), plasticity index (PI), gravel, sand, fines content (silt and clay) ratios and bearing capacity are found and plotted. Each parameter indicates the number of data, ranges (maximum and minimum), average and standard deviation. These geostatistical data are summarized in Table 1. After that the data set was arranged, tabulated, digitized and georeferenced to analysis by ArcGIS 10.8 software to achieve digital maps.

Table 2. Statistical Parameters of Geotechnical Properties of The Study Area.

		Gravel %	Sand %	Fines %	LL %	PI %	Bearing Capacity kN/m²
Depth 0.5-1.5 m	No. of data	63.0	63.0	63.0	82.0	82.0	106.0
	Max	82.4	46.0	99.0	59.9	30.2	207.0
	Min	0.0	1.0	6.0	18.0	5.0	56.0
	Mean	22.0	17.7	60.3	45.2	15.2	112.2
	Std. deviation	24.5	12.2	29.8	7.3	6.3	36.8
Depth 1.5-3.0 m	No. of data	83.0	83.0	83.0	71.0	71.0	114.0
	Max	80.0	45.0	96.0	59.2	30.5	321.0
	Min	0.0	0.0	4.4	16.0	3.0	80.0
	Mean	35.0	20.3	44.8	39.9	14.5	168.5
	Std. deviation	28.3	11.7	30.7	12.4	7.5	51.4
Depth 3.0-5.0 m	No. of data	82.0	82.0	82.0	59.0	59.0	108.0
	Max	84.0	54.0	96.0	56.0	27.4	417.0
	Min	0.0	0.0	2.3	18.0	3.0	116.0
	Mean	41.7	17.3	40.9	32.7	10.3	244.2
	Std. deviation	29.3	11.2	28.1	11.5	5.0	70.0

3.2. Interpreting Data for Bearing Capacity Calculation

In the most geotechnical reports, standard penetration test (SPT) is given, while dynamic cone penetration (DCP) is provided in some other reports. All values of SPT and DCP were converted to bearing capacity.

According to (Meyerhof, 1956), the allowable bearing capacity for 25mm settlement can be obtained from SPT-N value using Equation (1):

$$q_a = \frac{N}{0.08}\left(\frac{B+0.3}{B}\right)^2 \times w_\gamma \times R_d \quad (1)$$

Where, q_a = allowable bearing capacity kN/m², N = SPT blow number, w_γ= water table correction factor = $0.5 + 0.5\frac{b}{B} \leq 1$, b = depth of water table below the base (m), B = base width of footing (m), for this research B is taken as 2 m, R_d = depth correction factor = $1 + 0.33\frac{D_f}{B} \leq 1.33$, D_f = foundation depth (m).

Some of the geotechnical reports utilized DCP instead of SPT for determining the bearing capacity of cohesive soil (Alshkane et al., 2020) proposed Equation (2) where Unconfined Compressive Strength (UCS) is derived from the DCP.

$$UCS = 1033.6\, DCP^{-0.968} \quad (2)$$

Bearing capacity of the soils was calculated according to Equation (3) developed by (Terzaghi et al., 1996), for a foundation of undrained saturated soil when internal friction angles are zero.

$$q_u = 5.7 \times c_u + \gamma \times D_f \quad (3)$$

Where, q_u = ultimate bearing capacity (kN/m²), c_u = undrained shear strength (kN/m²), γ = unit weight of soil (kN/m³).

The allowable bearing capacity can be obtained by dividing the found ultimate bearing capacity by a factor of safety. The minimum factor of safety that can be used is 3.

3.3. Software and Management

The collected data were tabulated (sorted and categorized) in Microsoft Excel software which is recognized by the GIS environment. This includes the name of the studied site and the site's features. The borehole locations are spatially determined using base maps (imagery with labels) in ArcMap 10.8.

For the purpose of data analysis and production of digital maps, the method of kriging spatial-analyst interpolation tool is used.

4. Results and Discussions

According to the variation of geotechnical properties of the soil at the area, thematic maps have been driven for three different depths of the boreholes; 0.5-1.5, 1.5-3.0, and 3.0-5.0 m. In each depth, a digital map is achieved for soil bearing capacity, gravel percent, sand percent, fines percent, liquid limit, and plasticity index. They are divided into six classes and presented in different colors.

4.1. Particle Size

Particle size is one of the important parameters in soil classification, particle characteristics significantly influence the soil strength (Koerner, 1970). Generally, The angle of shearing resistance increases as the median particle diameter and gravel content increment (Wang et al., 2013). Fines content that includes silt and clay percentage of soil has a tremendous influence on the value of the soil strength and its settlement. Dominant fine content has higher plasticity and compressibility, greater potential swelling and lower hydraulic conductivity (Mitchell et al., 2005).

Figure 2a, 2b, and 2c show the variation of the gravel across the study area in the depths of 0.5-1.5, 1.5-3.0 and 3.0-5.0 m respectively. Average gravel content in the first, second and third layers are 22%, 35% and 41.7% respectively. The lowest gravel range is 0.0-12.8 % which is indicated in dark red color and it is found to be in the eastern part of the study area as shown in Figure 2a, while the gravel ratio increases gradually towards the western part that reaches the maximum range of 65.7- 76.7 % for the first layer. In the second layer, the dominant zone is the range of 42.2-61.1 % that depicted in light green color, also some small spots were created that included the maximum range of 61.2-75.4 % due to variation of the borehole values. However, the ranges of 32.6-42.1 % and below cover the north-east and the north-west parts, the gravel ratio increases moderately as illustrated in Figure 2b. In the third layer, the gravel ranges of 38.7-49.5 % and 49.6-60.4 % covered most parts of the studied area from the south to the north, although other ratios from the central to the border sides gradually decreased as displayed in amber to the dark red colors in Figure 2c.

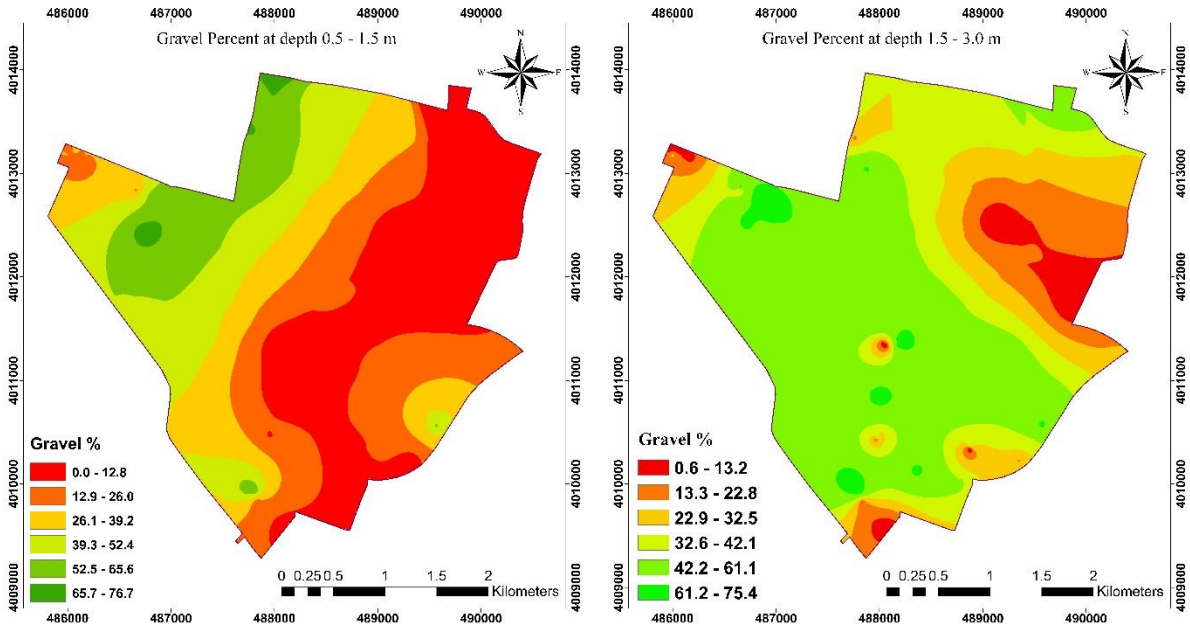

a) Gravel Ratio at Depth 0.5-1.5 m.

b) Gravel Ratio at Depth 1.5-3.0 m.

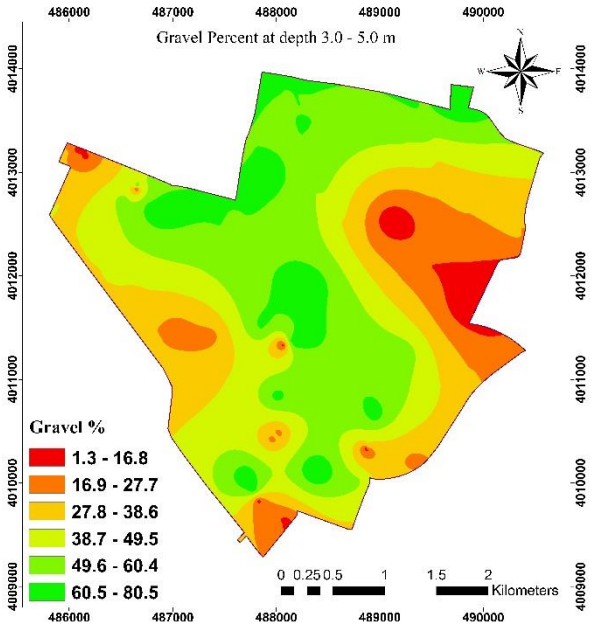

c) Gravel Ratio at Depth 3.0-5.0 m.

Figure 2. Distribution of Gravel Content with Depth a) 0.5-1.5 m, b) 1.5-3.0 m, and c) 3.0-5.0 m.

The average sand contents are 17.7%, 20.3% and 17.3% in all the three layers sequentially. Its ratio increased by 15% in the second layer compared to that of the first layer, while in the third layer the ratios are not significantly changed. Generally, the majority areas in all layers of sand percent covered by yellow and light brown colors with different patterns. Other ratios have been covered by a small area for each of depths, which are mostly available in the surrounding of the study area as in the Figure 3a, 3b, and 3c.

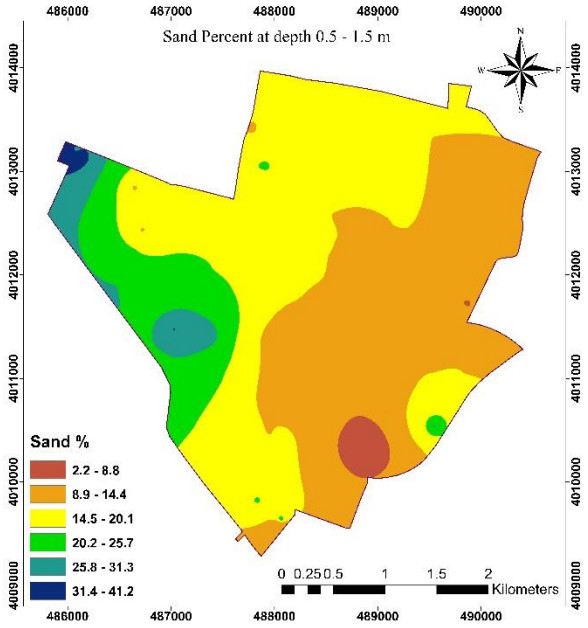

a) Sand Ratio at Depth 0.5-1.5 m.

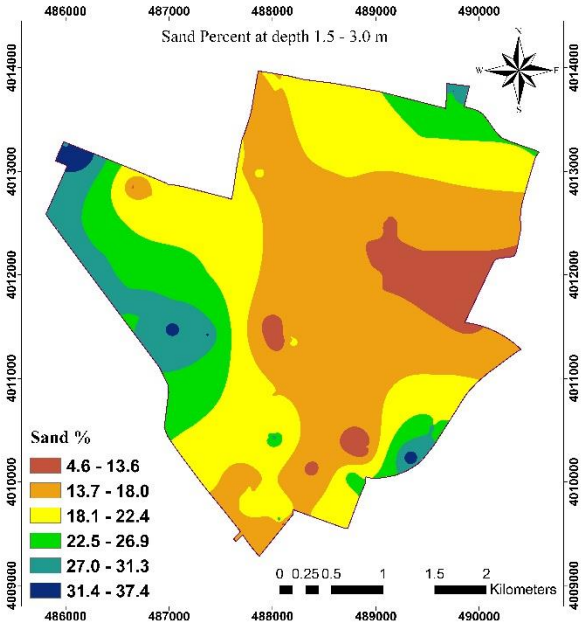

b) Sand Ratio at Depth 1.5-3.0 m.

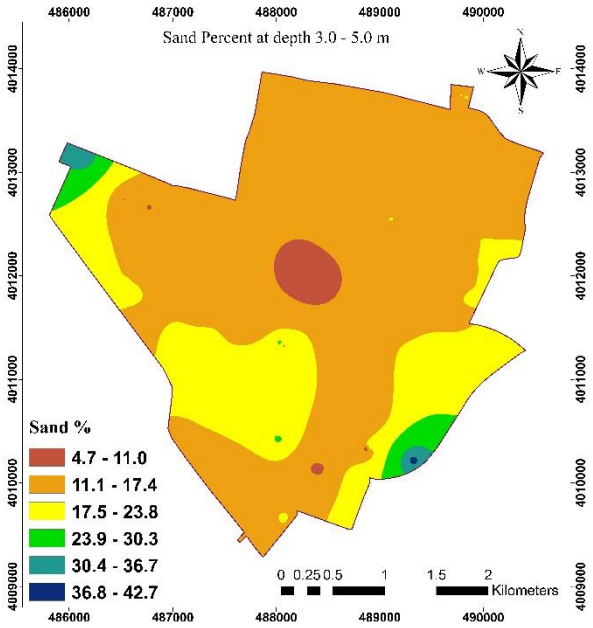

c) Sand Ratio at Depth 3.0-5.0 m.

Figure 3. Distribution of Sand Content with Depth a) 0.5-1.5 m, b) 1.5-3.0 m, and c) 3.0-5.0 m.

In the first layer, most of the study area can be considered as cohesive soil with the average fines content of 60.3% as demonstrated in dark blue, blue and green colors. It can be noticed from Figure 4a the fines content gradually increases toward the east of the study area, since the region is plain and agricultural land. In the second and third layers, fines content decreases compared to that of the first layer as the ratio decreases to 25.7% and 32.2% respectively. Predominant values of the second and third layers are represented in light brown and yellow colors zone as shown in Figure 4b and 4c.

To sum up, gravel dramatically increases with an increase in the depth of the layers, while fines content decreases. On the other hand, sand content was nearly the same.

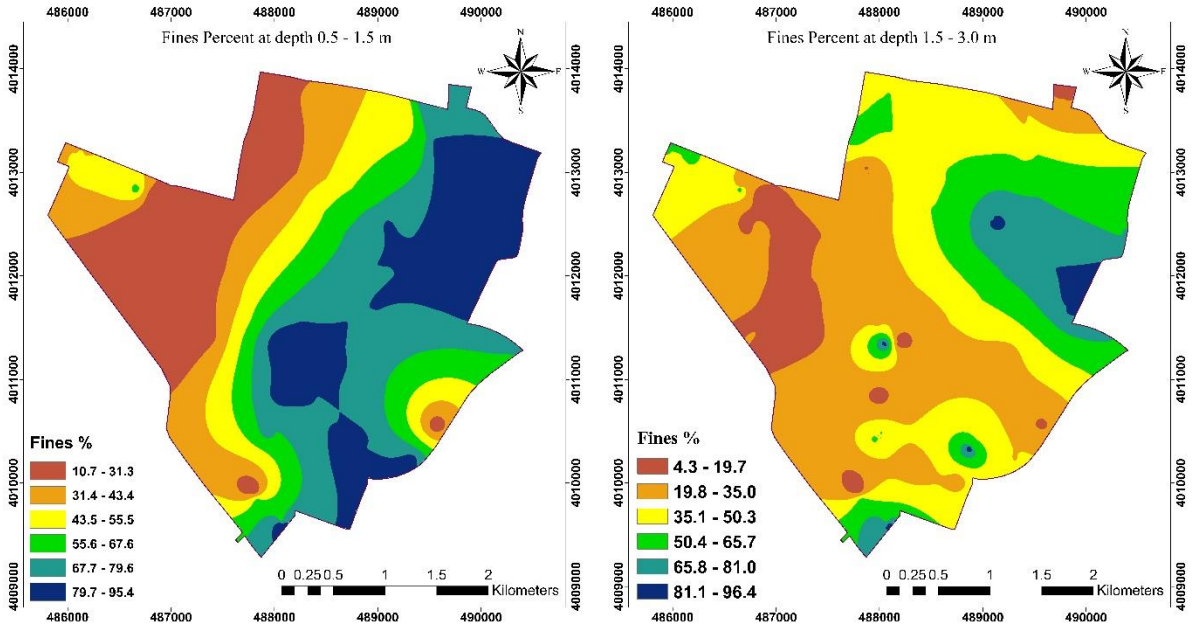

a) Fines Ratio at Depth 0.5-1.5 m.

b) Fines Ratio at Depth 1.5-3.0 m.

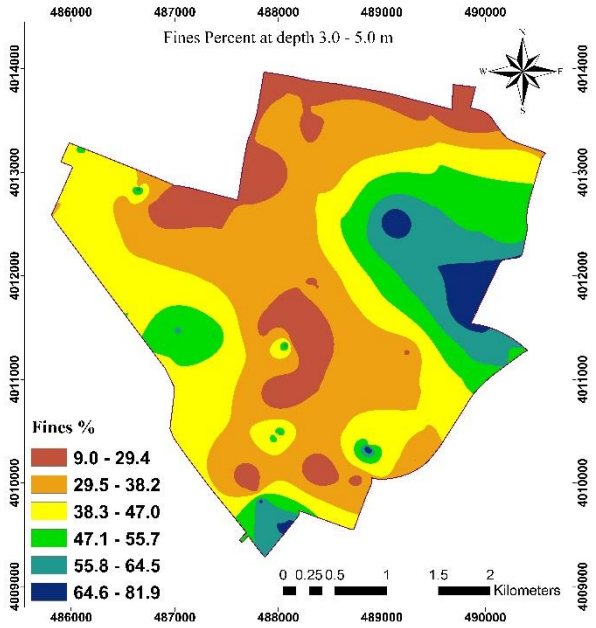

c) Fines Ratio at Depth 3.0-5.0 m.

Figure 4. Distribution of Fines Content with Depth a) 0.5-1.5 m, b) 1.5-3.0 m, and c) 3.0-5.0 m.

4.2. Atterberg Limits

The Atterberg limits are used to classify fine grain soil and to investigate some other geotechnical characteristics of soil such as compression index, soil shrinkage rate and swelling potential (Zhou and Lu, 2021). According to the gathered data from different boreholes, the values of the liquid limit and plasticity index in the study area vary from a place to another as displayed in Figure 5 and 6. The highest liquid limit value of 49.9-57.4 % is observed in the depth of 1.5-3.0 m, which is hatched in dark blue color in Figure 5b. However, the lowest liquid limit value of 17.5-24.5 % is observed at the south-east of the study area at the same depth, which is hatched in dark brown color that covers a small area. The dark blue color in Figure 5a indicates a high liquid limit range of 49.3- 57.1 %. In Figure 5b the majority of the area in the depth of 1.5- 3.0 m is hatched in dark blue color in the middle, north and west of the study area which is high liquid limit area. The low value of liquid limit ranged from 20.0-27.8 %, it can be noticed in the depth of 3.0-5.0 m of the area compared to two other depths as displayed in Figure 5c.

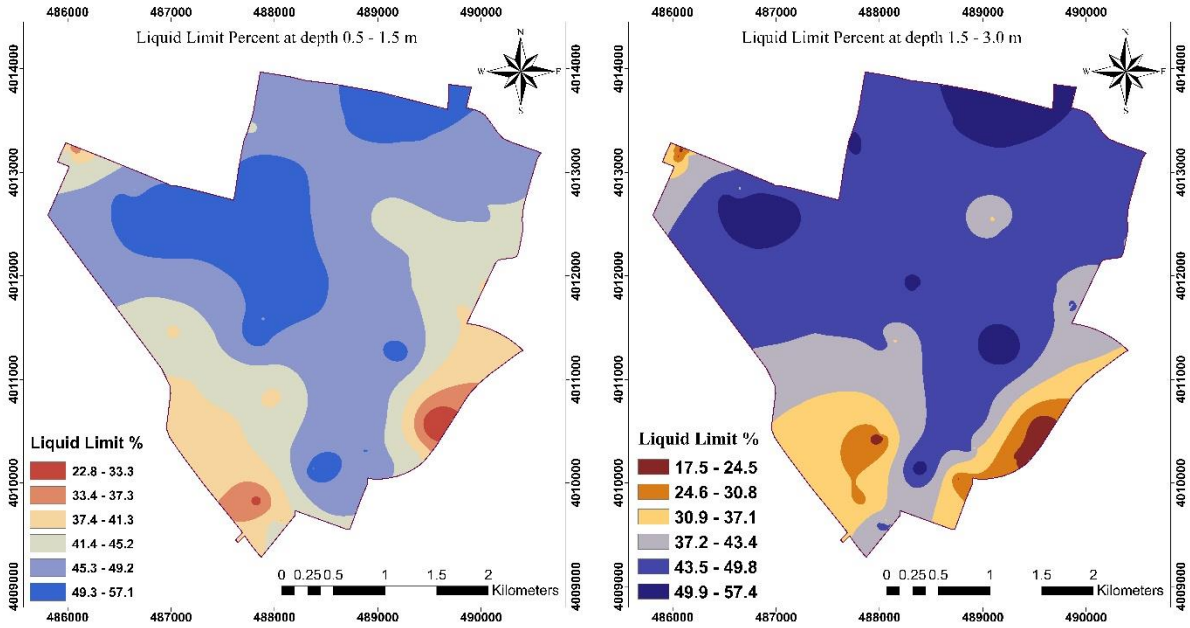

a) Liquid Limit % at Depth at 0.5-1.5 m. b) Liquid Limit % at Depth at 1.5-3.0 m.

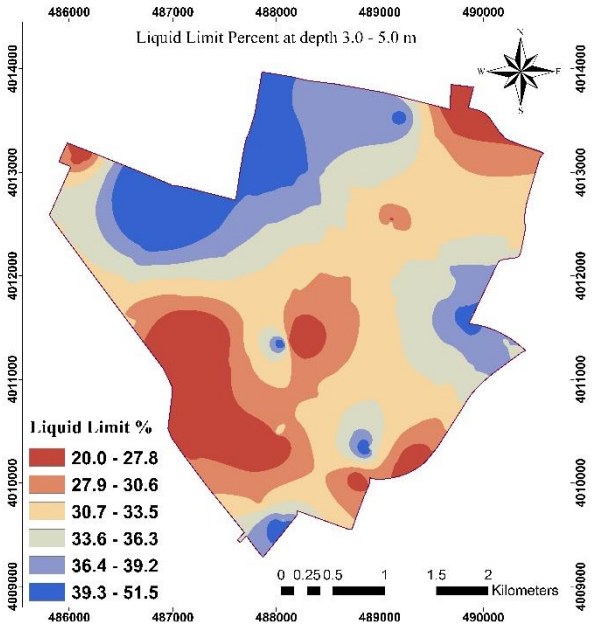

c) Liquid Limit % at Depth at 3.0-5.0 m.

Figure 5. Liquid Limit Distribution with Depth a) 0.5-1.5 m, b) 1.5-3.0 m, and c) 3.0-5.0 m.

Similar to the liquid limit values, the plasticity index (PI) percentage which is the difference between liquid limit and plastic limit varies from a place to another in the study area. The lowest percentage of PI of 3.9-7.3 % is noticed in depth of 1.5-3.0 m which is in the south part as indicated in Figure 6b and is hatched as light-yellow color. However, the highest percentage of PI of 26.0-29.1 % is observed at the same depth in the north part of the studied area. This range is hatched in dark brown color. The PI value is high in the north to the center of the area while it becomes lower in the south to the east in all depths. It is low in the depth of 3.0-5.0 m in the most of the studied area as shown in Figure 6c.

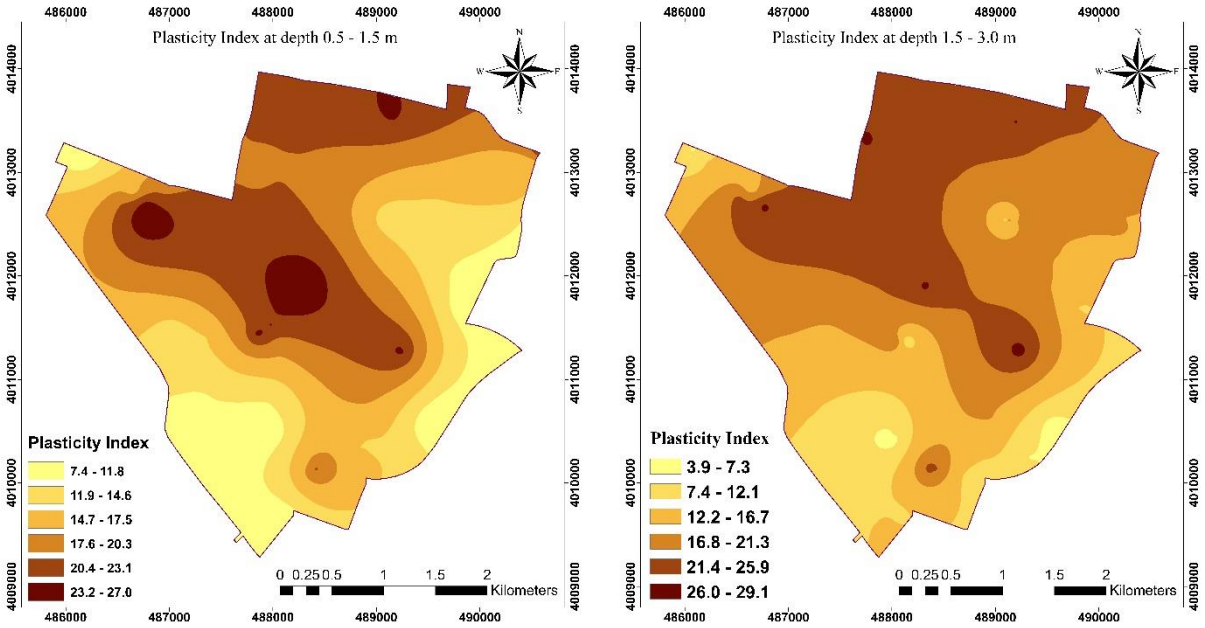

a) Plasticity Index % at Depth at 0.5-1.5 m. b) Plasticity Index % at Depth at 1.5-3.0 m.

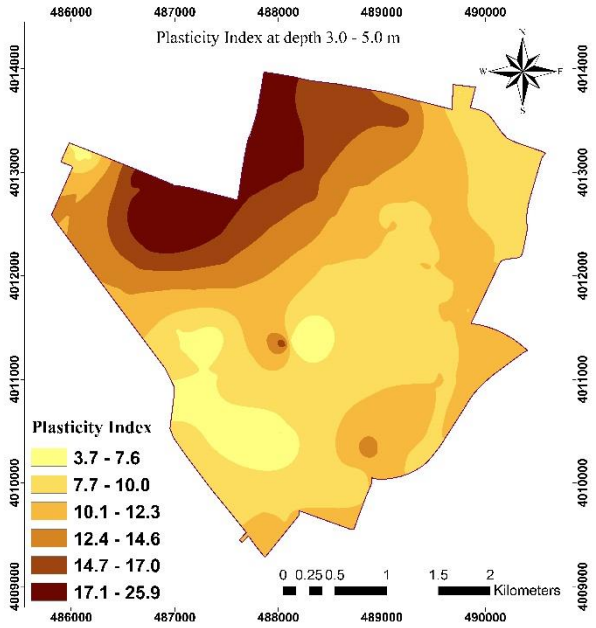

c) Plasticity Index % at Depth at 3.0-5.0 m.

Figure 6. Plasticity Index Distribution with Depth a) 0.5-1.5 m, b) 1.5-3.0 m, and c) 3.0-5.0 m.

4.3. Bearing Capacity

Bearing capacity changes horizontally and vertically across the thematic maps. The bearing capacity increases with an increase in the depth of the layer. Figure 7a shows the bearing capacity at a depth of 0.5-1.5 m. The dark blue color represents the high bearing capacity areas which mostly covers the southern and northern areas of the study. The highest range of the bearing capacity of that layer is between 143.1-182.4 kN/m². The eastern area has the minimum bearing capacity ranging from 74.7 to 95.3 kN/m². This is shown in red color that gradually changes to the orange and yellow colors pointing to the increase of bearing capacity toward the west.

In the depth of 1.5-3.0 m, the abundant range of bearing capacity is 157.0-182.6 kN/m², which is represented by yellow color. The orange color zone in Figure 7b represents the lower range of bearing capacity between 131.3 to 156.9 kN/m² that is extended from east to the north west of the study area. Due to the variation of soil properties, three areas show the highest value of bearing capacity in that layer in light blue color with the range of 182.7-208.2 kN/m².

The third layer which is at a depth of 3.0-5.0 m is depicted in Figure 7c and mainly hatched by two bearing capacity zones. The first zone is orange with bearing capacity of 213.2-239.4 kN/m² which is located in the east, west, and south. The second zone is yellow with bearing capacity of 239.5-265.6 kN/m² that is located in the center of the study area. The bearing capacity gradually increases until it reaches the maximum range of 318.2-365.9 kN/m² at the northern areas.

The thematic maps indicate that the bearing capacity increases with an increase in the depth of the layers. The bearing capacity at the second layer increases by approximately 33% compared to that of the first layer, while the bearing capacity at the third layer increases by about 31% compared to that of the layer above. Overall, the bearing capacity of the east side of the study area is lower than the other zones due to low ranges of gravel content about 0-16 % and sand content by 2-14 % and high fines content ranges 65-82 %. Moreover, in the north-west zone of the depth of 0.5-1.5 m, low bearing capacity achieved as shown in Figure 7a, due to high liquid limit rage 45-57 % and plasticity index ratios range 20-27 % while the gravel percent of same area is at its their range 52-76 %, Also, the same phenomena can also be noticed in the 3.0-5.0 m depth.

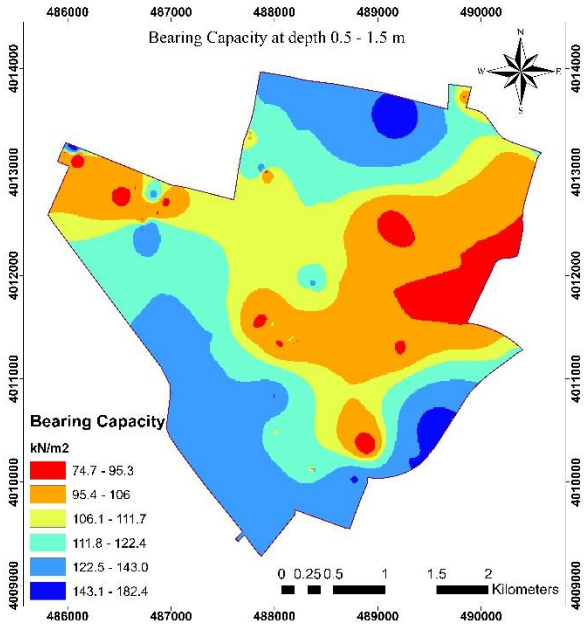

a) Bearing Capacity at Depth 0.5-1.5 m.

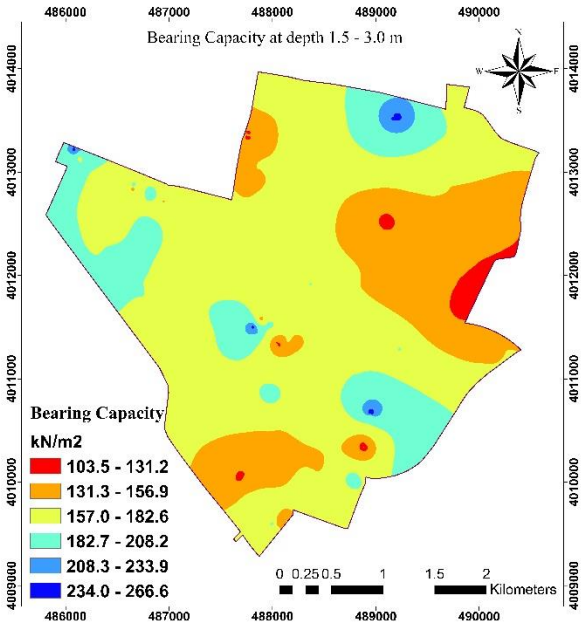

b) Bearing Capacity at Depth 1.5-3.0 m.

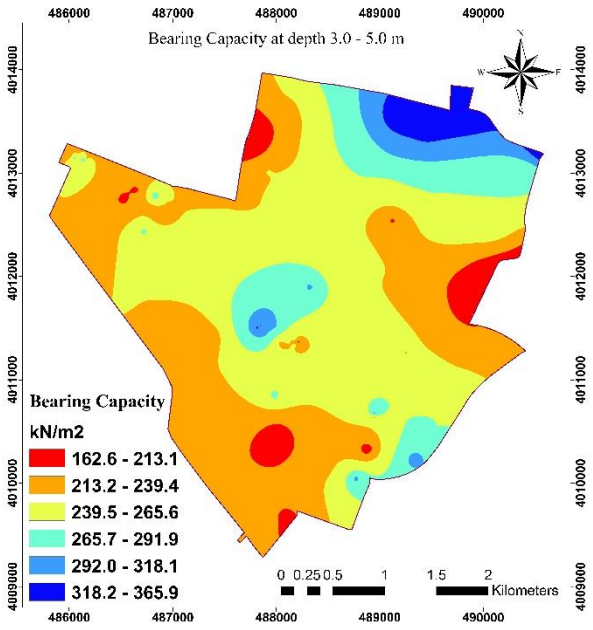

c) Bearing Capacity at Depth 3.0-5.0 m.

Figure 7. Spatial Bearing Capacity with Depth a) 0.5-1.5 m, b) 1.5-3.0 m, and c) 3.0-5.0 m.

5. Conclusions

This research focuses on creating digital geotechnical maps by using ArcGIS software and natural neighboring interpolation. The investigation relies on data of 116 boreholes distributed over an area of 13.02 km² as the study area from geotechnical reports collected from 26 sites in Ranya city, Iraq. These are main conclusions:

1) GIS is a useful tool for capturing, displaying and analyzing geographically referenced data.
2) The maps show that with an increase in depth of the layer in Ranya soil, average gravel percentage increases by 59% in the second layer, and approximately doubled in the third layer by 89.6% compared to the first layer. Also average fines content decreases in the second and third layers by about 25.7% and 32.2% lower than the first layer, respectively while the sand content remains nearly the same.
3) Liquid limit decreased according to the first layer about 12% and 28% in the second and third layer, respectively. Plasticity index in the second layer almost remain the same and in the third layer reduces 32% compared to the first layer. Based on the maps for LL and PI, the liquid limit and plasticity index reduce from the north to south with an increase in the depth of the third layer. The highest liquid limit value of 49.9-57.4 % is observed in the second layer. However, the lowest liquid limit value of 17.5-24.5 % is observed at the south-east of the study area at the same depth. Plasticity index is similar to LL and declined from the north to the south. The lowest percentage of PI of 3.9-7.3 % is noticed in the second layer which is in the south. However, the highest percentage of PI of 26.0-29.1 % is observed at the same depth in the north part of the studied area.
4) According to the created maps for bearing capacity, high bearing capacity areas are mostly located in the southern and northern area of Ranya. However, the eastern area has the minimum bearing capacity which gradually increases towards the west.
5) The thematic maps indicate the fact that bearing capacity increased with depth. The value in the second depth increased by approximately 33% and the value in the third depth increased by 54% in comparison to the first layer. The low bearing capacity in northwest zone of the area is achieved due to the high consistency limits, and the high percentage of gravel content which ranges between 52.5-65.6%, and the same phenomena can also be noticed in the third layer.

Acknowledgments

The authors would like to specially thank Sulaimani general construction laboratory staff, consultant engineering bureau of University of Sulaimani and directors of Raparin's administration that supported the authors and provided their unpublished data.

References

Ahmed, C., Mohammed, A., and Tahir, A. (2020). Geostatistics of strength, modeling and GIS mapping of soil properties for residential purpose for Sulaimani City soils, Kurdistan Region, Iraq. *Modeling Earth Systems and Environment*, 1–15. https://doi.org/https://doi.org/10.1007/s40808-020-00715-y

Al-Ani, H., Eslami-Andargoli, L., Oh, E., and Chai, G. (2013). Categorising geotechnical properties of surfers paradise soil using geographic information system (GIS). *International Journal of Geomate*, *5*(2), 690–695.

Al-Jiburi, H. K., and Al-Basrawi, N. H. (2015). Hydrogeological map of Iraq, scale 1: 1000 000, 2013. *Iraqi Bulletin of Geology and Mining*, *11*(1), 17–26.

Al-Maliki, L. A. J., Al-Mamoori, S. K., El-Tawel, K., Hussain, H. M., Al-Ansari, N., Al Ali, M. J., and others. (2018). Bearing capacity map for An-Najaf and Kufa cities using GIS. *Engineering*, *10*(05), 262.

Al-Mamoori, S. K., Al-Maliki, L. A. J., Al-Sulttani, A. H., El-Tawil, K., Hussain, H. M., and Al-Ansari, N. (2020). Horizontal and vertical geotechnical variations of soils according to USCS classification for the city of An-Najaf, Iraq using GIS. *Geotechnical and Geological Engineering*, *38*(2), 1919–1938. URL: https://doi.org/https://doi.org/10.1007/s10706-019-01139-x

Al-Manmi, D. A. A. (2008). Water resources management in Rania area, Sulaimaniyah NE-Iraq. *College of Science, University of Baghdad*, *PhD Thesis*, 225 p.

Aldefae, A. H., Mohammed, J., and Saleem, H. D. (2020). Digital maps of mechanical geotechnical parameters using GIS. *Cogent Engineering*, *7*(1), 1779563. URL: https://doi.org/https://doi.org/10.1080/23311916.2020.1779563

Ali, H. M., and Shakir, R. R. (2021). Geotechnical map of Thi Qar governorate using geographical information systems (GIS). *Materials Today: Proceedings*. URL: https://doi.org/https://doi.org/10.1016/j.matpr.2021.09.138

Alshkane, Y. M., Rashed, K. A., and Daoud, H. S. (2020). Unconfined Compressive Strength (UCS) and Compressibility Indices Predictions from Dynamic Cone Penetrometer Index (DCP) for Cohesive Soil in Kurdistan Region/Iraq. *Geotechnical and Geological Engineering*, *38*(4), 3683–3695. URL: https://doi.org/https://doi.org/10.1007/s10706-020-01245-1

Annual population statistical report[PDF]. (2021). *Iraqi Kurdistan Regional Government, Ministry of Planning, Raparin Statistics Directorate, Ranya*.

Arshid, M. U., and Kamal, M. A. (2020). Regional geotechnical mapping employing kriging on electronic geodatabase. *Applied Sciences*, *10*(21), 7625. URL: https://doi.org/https://doi.org/10.3390/app10217625

ASTM, D. 422-63. (2007). Standard test method for particle-size analysis of soils. *West Conshohoken, PA: ASTM International*, *04.08*, 10–17.

ASTM, D. 4318. (2010). Standard test methods for liquid limit, plastic limit, and plasticity index of soils. *ASTM International, West Conshohocken, PA*.

ASTM D D6951. (2003). *Standard test method for use of the dynamic cone penetrometer in shallow pavement applications*.

ASTM D1586-11. (2011). Standard test method for standard penetration test (SPT) and split-barrel sampling of soils. *ASTM Standard Test Method,* 1–9.

ASTM D7263. (2018). Standard Test Methods for Laboratory Determination of Density and Unit Weight of Soil Specimens. *United States: American Society for Testing and Material.*, *i*(March), 1–7. https://doi.org/10.1520/D7263-09R18E02

Bapeer, G. B., Muhammad, R. K., Nadr, K. A., Khodakarami, L., and Al-Ansari, N. (2020). Geotechnical Properties of Soil in Ranya and Arbat Area, Sulaimaniya, Kurdistan Region, Iraq. *Journal of Earth Sciences and Geotechnical Engineering*, *10*(5), 35–48.

Cabalar, A. F., Karabas, B., Mahmutluoglu, B., and Yildiz, O. (2021). An IDW-based GIS application for assessment of geotechnical characterization in Erzincan, Turkey. *Arabian Journal of Geosciences*, *14*(20), 1–14. URL: https://doi.org/https://doi.org/10.1007/s12517-021-08481-6

Celik, F., Öztürk, M. Z., Sener, M. F., Ariöz, Ö., and Erbil, M. (2021). Mapping investigation based on engineering geology of a developing urban area (Nigde, Turkey). *Arabian Journal of Geosciences*, *14*(14), 1–17. URL: https://doi.org/https://doi.org/10.1007/s12517-021-07699-8

Consultant Engineering Bureau of Sulaimani University. (n.d.). *Geotechnical Investigation Reports, Iraqi Kurdistan Regional Government, Ministry of Higher Education and Scientific Research, University of Sulaimani, College of Engineering, Consultant Engineering Bureau.*

El-Kady, M. S., and ElMesmary, M. A. (2018). Creating spatial database of the foundation soil in Aljouf area using GIS. *Innovative Infrastructure Solutions*, *3*(1), 1–6. URL: https://doi.org/https://doi.org/10.1007/s41062-018-0155-2

Jassim, S. Z., and Goff, J. C. (2006). *Geology of Iraq*. DOLIN, sro, distributed by Geological Society of London.
Jimenez, M. J., Garcia-Fernandez, M., Zonno, G., and Cella, F. (2000). Mapping soil effects in Barcelona, Spain, through an integrated GIS environment. *Soil Dynamics and Earthquake Engineering*, *19*(4), 289–301. URL: https://doi.org/https://doi.org/10.1016/S0267-7261(00)00007-5
Kadhim, K. N., and Al-Abody, A. A. M. (2015). The geotechnical maps for bearing capacity by using GIS and quality of ground water for Al-Imam District (Babil-Iraq). *International Journal of Civil Engineering and Technology*, *6*(10), 176–184.
Kadhim, M. M., Al-Saoudi, N. K. S., and Ziboon, A. R. T. (2013). Digital geotechnical maps of Basrah city using geographical information systems technique. *Engineering \& Technology Journal*, *31*, 599–617.
Kamal, M. A., Arshad, M. U., Khan, S. A., Zaidi, B. A., and others. (2016). Appraisal of geotechnical characteristics of soil for different zones of Faisalabad (Pakistan). *Pakistan Journal of Engineering and Applied Sciences*.
Kaur, L., Garg, P., and Grewal, G. K. (2019). Bearing Capacity Mapping of Srinagar, J&K. In *International Conference on Sustainable Waste Management through Design* (pp. 449–454). URL: https://doi.org/10.1007/978-3-030-02707-0_51
Khalid, M. H., Alshameri, B., and Abid, U. (2021). Application of Kriging for development of SPT N value contour maps and USCS-based soil type qualitative contour maps for Islamabad, Pakistan. *Environmental Earth Sciences*, *80*(11), 1–13. URL: https://doi.org/https://doi.org/10.1007/s12665-021-09720-5
Khdir, S. H., and Saeed, K. T. (2021). Landfill Site Selection Using GIS and (AHP): Case Study of Ranya City. *Academic Journal of Nawroz University*, *10*(4), 39–49.
Koerner, R. M. (1970). Effect of particle characteristics on soil strength. *Journal of the Soil Mechanics and Foundations Division*, *96*(4), 1221–1234. URL: https://doi.org/https://doi.org/10.1061/JSFEAQ.0001436
Labib, M., and Nashed, A. (2013). GIS and geotechnical mapping of expansive soil in Toshka region. *Ain Shams Engineering Journal*, *4*(3), 423–433. URL: https://doi.org/https://doi.org/10.1016/j.asej.2012.11.005
Manguri, S. B. H., and Hamza, A. A. (2021). Sanitary Landfill Site Selection Using Spatial-AHP for Pshdar Area, Sulaymaniyah, Kurdistan Region/Iraq. *Iranian Journal of Science and Technology, Transactions of Civil Engineering*, 1–14. URL: https://doi.org/https://doi.org/10.1007/s40996-021-00605-y
Meyerhof, G. G. (1956). Penetration tests and bearing capacity of cohesionless soils. *Journal of the Soil Mechanics and Foundations Division*, *82*(1), 861–866. URL: https://doi.org/https://doi.org/10.1061/JSFEAQ.0000001
Mirzahossein, H., Sedghi, M., Habibi, H. M., and Jalali, F. (2020). Site selection methodology for emergency centers in Silk Road based on compatibility with Asian Highway network using the AHP and ArcGIS (case study: IR Iran). *Innovative Infrastructure Solutions*, *5*(3), 1–14. URL: https://doi.org/https://doi.org/10.1007/s41062-020-00362-3
Mitchell, J. K., Soga, K., and others. (2005). *Fundamentals of soil behavior* (Vol. 3). John Wiley \& Sons New York.
Mohammed, M. S., Hasan, M. F., and Al-bayati, K. S. (2020). Geotechnical maps for Salah Al-Deen-Iraq. *IOP Conference Series: Materials Science and Engineering*, *737*(1), 12224.
Najmaddin, P. M., Salih, N. B., and Abdalla, T. A. (2020). Evaluating the Spatial Distribution of some Soil Geotechnical Properties Using Various Interpolation Methods (Case Study: Sulaimani Province, Iraq). *Journal of Soil Sciences and Agricultural Engineering*, *11*(7), 275–281. URL: https://doi.org/DOI: 10.21608/JSSAE.2020.109461
Rashed, K. A., and Hussein, A. A. (2020). GIS as A Tool for Expansive Soil Detection at Sulaymaniyah City. *Journal of Engineering*, *26*(6), 152–171.
Razmyar, A., and Eslami, A. (2016). Geotechnical Zoning of Municipal Districts 4 and 22 of Great Tehran. *2nd International Conference on Research in Civil Engineering, Architecture, Urban Planning and Sustainable Environment*.
Razmyar, A., and Eslami, A. (2018). Evaluating the geotechnical and geophysical characteristics of expanding districts in Tehran using field experiments. *Civil Engineering Journal*, *4*(2), 363–377.
Seko Private Construction Lab. (n.d.). *Geotechnical Investigation Reports, Seko Private Construction Laboratory, Sulaymaniyah, Iraq*.
Singh, A., Noor, S., Chitra, R., Gupta, M., and Vel, N. K. (2015). GIS applications in geotechnical engineeringsome case studies. *International Journal of Latest Trends in Engineering and Technology*, *5*(2).
Sissakian, V. K. (2000). Geological Map of Iraq, 3rd edit., scale 1: 1000 000. *GEOSURV, Baghdad, Iraq*.
Sulaymaniyah General Construction Lab. (n.d.). *Geotechnical Investigation Reports, Iraqi Kurdistan Regional Government, Ministry of Construction and Housing, Sulaymaniyah General Construction Laboratory*.
Terzaghi, K., Peck, R. B., and Mesri, G. (1996). *Soil mechanics in engineering practice* (3rd editio). John Wiley \& Sons.
Tripathi, S. M., Chaurasia, S., and Sharma, P. K. (2021). Detection Prediction and Mapping of Chromium through QGIS and Adsorption of Hexavalent Chromium by Modified Bio-Adsorbents: Kinetic and Adsorption study. *Innovative Infrastructure Solutions*. URL: https://doi.org/https://doi.org/10.1007/s41062-021-00563-4
Valverde-Palacios, I., Valverde-Espinosa, I., Irigaray, C., and Chacón, J. (2014). Geotechnical map of Holocene alluvial

soil deposits in the metropolitan area of Granada (Spain): a GIS approach. *Bulletin of Engineering Geology and the Environment*, *73*(1), 177–192. URL: https://doi.org/https://doi.org/10.1007/s10064-013-0540-1

Wang, J.-J., Zhang, H.-P., Tang, S.-C., and Liang, Y. (2013). Effects of particle size distribution on shear strength of accumulation soil. *Journal of Geotechnical and Geoenvironmental Engineering*, *139*(11), 1994–1997. URL: https://doi.org/https://doi.org/10.1061/(ASCE)GT.1943-5606.0000931

Zhou, B., and Lu, N. (2021). Correlation between Atterberg limits and soil adsorptive water. *Journal of Geotechnical and Geoenvironmental Engineering*, *147*(2), 4020162. URL: https://doi.org/https://doi.org/10.1061/(ASCE)GT.1943-5606.0002463